A STUDY ON ANOMALOUS SIGNAL DETECTION USING HMM FOR ELF ELECTROMAGNETIC WAVE

Yoshinao ITO, Akitoshi ITAI*, Hiroshi YASUKAWA*, Ichi TAKUMI† and Masayasu HATA‡*

Aichi Prefectural University*, Nagoya Institute of Technology†, Chubu University‡
Faculty of Information Science and Technology*, Faculty of Engineering†, Collage of Engineering‡
Ibaragabasama Kumabari Nagakute-cho Aichi*, Gokiso-cho showa-ku Nagoya-shi Aichi†, Matsumoto-cho Kasugai-shi Aichi‡

1. INTRODUCTION

Anomalous radiations of EM waves due to an earth diastrophism has been recorded in advance of earthquakes and volcanic activities[1]. We have been measuring the EM wave radiation in the ELF band. Our research is directed towards identifying an anomalous radiation of earthquakes from the EM wave data[2]. Observed signals contain undesired components associated with the magnetosphere, the ionized layer and the lightning radiation in the tropics, and so on[3]. Various signal processing techniques have been proposed to detect and understand the anomalous radiation in the ELF band.

The normal value method[4] and the principal component analysis[5] is proposed as the simple anomalous signal detection. These methods require the observation signal of several years at the same observation point. It is difficult to detect the anomalous signal in a new observation point. The neural network[6] is applied to overcome the weakness of conventional methods. The neural network approach does not require the observed signal recorded over several years at the same observation point. However, in order to achieve the accurate detection, many anomalous signals corresponding to the great earthquake are necessary for the training data set. The anomalous signal detection using a linear prediction error can detect seismic signal without anomalous signals. This technique detects abrupt noises as anomalous signals.

Requirements for an anomalous signal detection are outlined below: (i) An anomalous signal can be detected from the data observed at various site. (ii) Decrease the number of anomalous signal as training signal. (iii) Decrease the false detection due to an abrupt noise.

In this paper, the HMM is applied as the anomalous signal detection satisfying the above requirements. The HMM input signal the amplitude density distribution calculated from the waveform of the EM wave data excluding the anomalous signal. The training data is observed at various seasons and observation points. The observation signal including the abrupt noise is also used as training data to avoid the false detection. Results of the anomalous signal detection will indicate different characteristics when the display scale of the waveform is changed. The number of states of HMM influences the anomalous signal detection accuracy. This paper represents the optimal display scale of the image and the number of state of HMM, and shows possibility anomalous signal can be detected before earthquake occurred.

2. ELECTROMAGNETIC WAVE IN ELF BAND

We observed the EM wave radiation in the ELF band (223Hz) as represented by the east-west, north-south, and vertical magnetic field components at about forty observation stations in Japan. Collected data is averaged over 6 seconds interval (14400 points per day) at each station and direction. The EM wave data averaged over 6 and 150 seconds interval is recorded on the data logger established in Nagoya Institute of Technology. The data server provides us the numerical data and its graphical image.

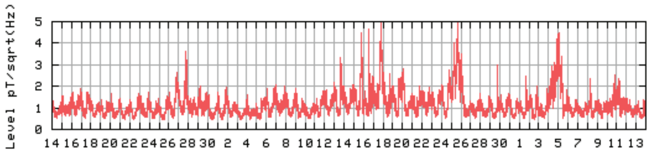

Fig. 1. Observed EM wave

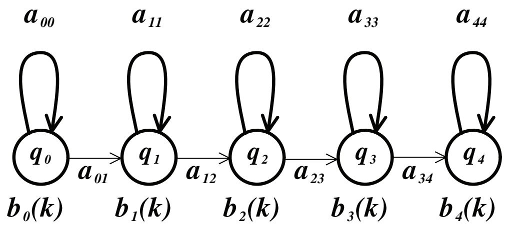

Fig. 2. State transition diagram for a 5-state left-to-right HMM

The typical seismic radiation from the earth's crust observed in the ELF band has a field strength of about on a pico Tesla normalized by the square root of one frequency $(\mathrm{pT}/\sqrt{\mathrm{Hz}})$.

A signal observed at Aomori-Hachinohe station is shown in Fig.1. The vertical axis represents a density of a magnetic flux $(\mathrm{pT}/\sqrt{\mathrm{Hz}})$, the horizontal axis indicates the time. The right-hand side origin is set to 0:00 AM, August 13th, 2001. An earthquake occurred on the 13th of August 2001. We can see the anomalous signal where about 5th August and 25th July.

Our goal is to detect the $P(t)$ accurately. This paper employs the two types of observed data. One includes the anomalous, another does not contain the $P(t)$. The former expressed as $T(t) + P(t) + w(t)$ is called as anomalous pattern, the latter represented by $T(t) + w(t)$ is referred as a normal pattern.

3. HIDDEN MARKOV MODEL

In this paper, HMM is applied to detect the anomalous signal from the EM wave data. HMM employed here forms the left-to-right type (Fig.2), and has the set of parameter, which consists of state q_i, state transition probability a_{ij} and observation symbol probability $b_j(k)$. Each parameter is estimated by using Baum-Welch algorithm and a normal pattern data. The trained HMM outputs a high-acceptance probability for a normal pattern, while a low-acceptance probability for an anomalous pattern.

4. INPUT OF HMM

Anomalous signals are detected by HMM that is trained by only normal pattern data. The amplitude density distribution of the EM wave data is used as a feature vector of HMM. The symbol is extracted from the waveform of the EM wave data released at a data server.

The flow of a symbol extraction is given as following steps: (i) Acquire the Graphics Interchange Format (GIF) file of EM wave data. (ii) Convert GIF image into the Microsoft Windows Bitmap (BMP) image. (iii) Extract the waveform area (Fig.3). (iv) Calculate the number of pixel, which include the waveform, at each line ($o = o_1 o_2 \cdots o_{86}$). (v) Input symbol $O = O_1 O_1 \cdots O_{86}$ is calculated by a normalizing coefficient S and o, as shown in (1). The input image and its observation symbol O is shown in Fig.4.

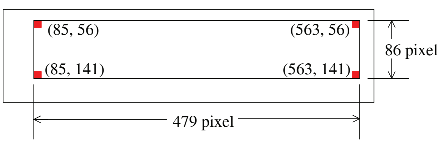

Fig. 3. Waveform area in the image of EM wave data

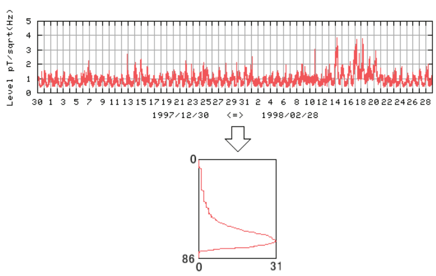

Fig. 4. Observed signal and input symbols

Table 1. Combination of training data and test data

training data	test data
ABCD	EF
ABCE	DF
ABDE	CF
ACDE	BF
BCDE	AF

$$S = \frac{\max o}{31}, \quad O = o \cdot S. \tag{1}$$

5. SIMULATION

5.1. Simulation I

The waveform of the EM wave data can be displayed on the following conditions.

- **X-axis**(Observation days): 1, 2, 7, 14, 30, 60 [days]
- **Y-axis**(Upper of density of magnetic flux): 3, 5, 10, 20, 50, 100, 200 [$pT/\sqrt{Hz}$]

Anomalous signals are often observed several weeks before an earthquake. These signals tend to decrease just before the earthquake. It is difficult to detect the anomalous signal from the image of X-axis 1 and 2 days. The image displayed on the scale on 7, 14, 30 and 60 days is used here. Almost of the normal signal is observed as less than 5 $pT/\sqrt{Hz}$. It is known that the EM wave data observed as more than 10 $pT/\sqrt{Hz}$, is the anomalous signal from an empirical knowledge. Therefore, as for the maximum value of Y-axis, more than 10 $pT/\sqrt{Hz}$ is unnecessary. The image displayed by 5 or 10 $pT/\sqrt{Hz}$ is employed.

Fifty data of a normal pattern and ten data of an anomalous pattern in each scale are prepared. Fifty normal patterns are divided into group A, B, C, D and E. Group A, B, C ,D and E include ten normal pattern data respectively Ten data of anomalous pattern are called group F. Four groups of normal patterns are given to HMM as training data. The group of a normal pattern not used and the group F are input to HMM that has been trained.

A threshold to distinguish a normal pattern and an anomalous pattern is the lowest value of the acceptance probability of the test normal patterns, and is calculated in each state. The false detection is defined as the number of the anomalous signal which yields larger acceptance probability than threshold. These calculations are processed five times as shown in Table 1. This process is repeated while changing the display scale of the image and the number of states of HMM.

The false detection rate with various image display scales and the number of states is shown in Table 2. There is the lowest false detection rate when the image of 14 days, 5 $pT/\sqrt{Hz}$, and the number of states is three. It pays attention to the result when the image of different Y-axis and the image of the same X-axis is used. At this time, 30 states of HMM satisfy that a false detection rate when the image displayed with 5 $pT/\sqrt{Hz}$ is less than its when the image displayed with 10 $pT/\sqrt{Hz}$. Therefore, the image displayed with 5 $pT/\sqrt{Hz}$ is effective to detect the anomalous signal since the false detection rate is less than the image displayed with 10 $pT/\sqrt{Hz}$.

5.2. Simulation II

Right hand side of anomalous patterns used in simulation I is the day when the earthquake is occurred. In this simulation, we evaluate how fast we can detect the anomalous signal. The same image of training data as the simulation I is prepared. The test data to which right and left hand side of image is set on -2, -4, -6, -8, -10, -12, -14[day](Fig.5). Those test data is same observation point as simulation I. Other conditions are the same conditions as simulation I.

The false detection rate with various image and the number of states is shown in Table 3. In Table 3, when X-axis is -2 and -8, there are the lowest false detection rate. This result shows the possibility that the anomalous signal can be detected before earthquake occurred.

6. CONCLUSION

We propose a new detection method of the anomalous signal related to an electromagnetic wave radiation using HMM. The amplitude density distribution of the observed data from the EM wave is adopted as the training data. It is shown that proposed method has a possibility of obtaining a good performance on the anomalous signal detection. And proposed method shows the possibility that the anomalous signal can be detected before earthquake occurred.

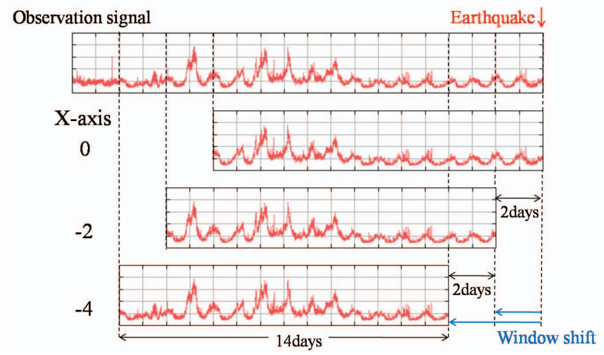

Fig. 5. Caluclate image for simulation II

Table 2. False detection rate(simulation I)

Scale of image X-axis [days]	Scale of image Y-axis $[pT/\sqrt{Hz}]$	1	2	3	4	5	6	7	8	9	10
		False detection rate [%] Number of state									
7	5	14	14	14	12	16	26	28	28	16	19
	10	18	42	22	26	38	20	14	18	24	26
14	5	2	28	0	2	4	8	8	10	14	16
	10	14	72	12	38	22	16	22	12	16	30
30	5	22	20	16	22	22	22	28	34	32	32
	10	16	44	20	36	18	18	22	28	32	16
60	5	40	56	40	42	42	44	48	54	54	56
	10	68	70	70	70	68	36	70	66	70	72

Table 3. False detection rate(simulation II)

Window shift from earthquake [day]	1	2	3	4	5	6	7	8	9	10
	False detection rate [%] Number of state									
-2	2	0	0	2	0	2	2	4	8	8
-4	14	14	16	12	14	16	16	16	20	20
-6	4	2	2	2	2	4	4	8	8	6
-8	0	0	0	0	0	0	4	10	16	14
-10	4	2	2	2	2	8	10	18	20	18
-12	14	16	18	16	10	18	20	10	18	20
-14	16	16	18	16	16	22	22	24	32	32

As a future works, we consider the more good condition of HMM, about number of state and image display scale.

7. REFERENCES

[1] M.B.Gokhberg, V.A.Morgunovm, T.Yoshio and I.Tomizawa: Experimental Measurements of Electromagnetic Emissions Possibly Relate to Earthquakes in Japan, Journal of Geophysical Research, 87, pp.7824-7829, 1982.

[2] M.Hata, I.Takumi, S.Adachi and H.Yasukawa: An Analytical Method to Extract Precursor from Noisy Atmospherics , Proc. of European Geophysical Society XXV, NH014, pp.25-29, 2000.

[3] M.Hata, I.Takumi and S.Yabashi: A Model of Earthquake Seen by Electromagnetic Observation - Gaseous Emission from the Earth as Main Source of Pre-Seismic Electromagnetic Precursor and Trigger of Followed Earthquake, Proceedings of European Geophysical Society, NH080, 1998.

[4] S.Niwa, H.Yaukawa, M.Hata and I.Takumi: A Signal Detection on Precursor of Earthquake Using Normal Value for ELF Electromagnetic Wave Observation, Proc. of Int. Sympo. on Information Theory and Its Applications, pp.863-866, 2002.

[5] S.Niwa, H.Yaukawa, M.Hata and I.Takumi: A Study on Precursor Signal Extraction with PCA for Predicting Significant Earthquakes, IEICE Trans. Fund., Vol.E86-A, No.8, pp.2047-2052, 2003.

[6] A.Itai, H.Yasukawa, I.Takumi and M.Hata: Anomalous Signal Detection in ELF Band Electromagnetic Wave using Multi-layer Neural Network with Wavelet Decomposition, IEEJ Trans. FM, Vol.129, No.12, pp.875-883, 2009.

Acknowledgment

This research was supported in part by JSPS for the Grant-in-Aid for Scientific Research (A)20246068.